

Figure S1

Showcases comparing proposed ratio of stalled reads (RSR) metric with coverage drop signal (CDS) metric used to resolve RNA G-quadruplex (rG4)-induced reverse transcriptase stalling (RTS) events at (a) *BASP1* gene (b) *EEF2* gene (c) *RPL13* gene

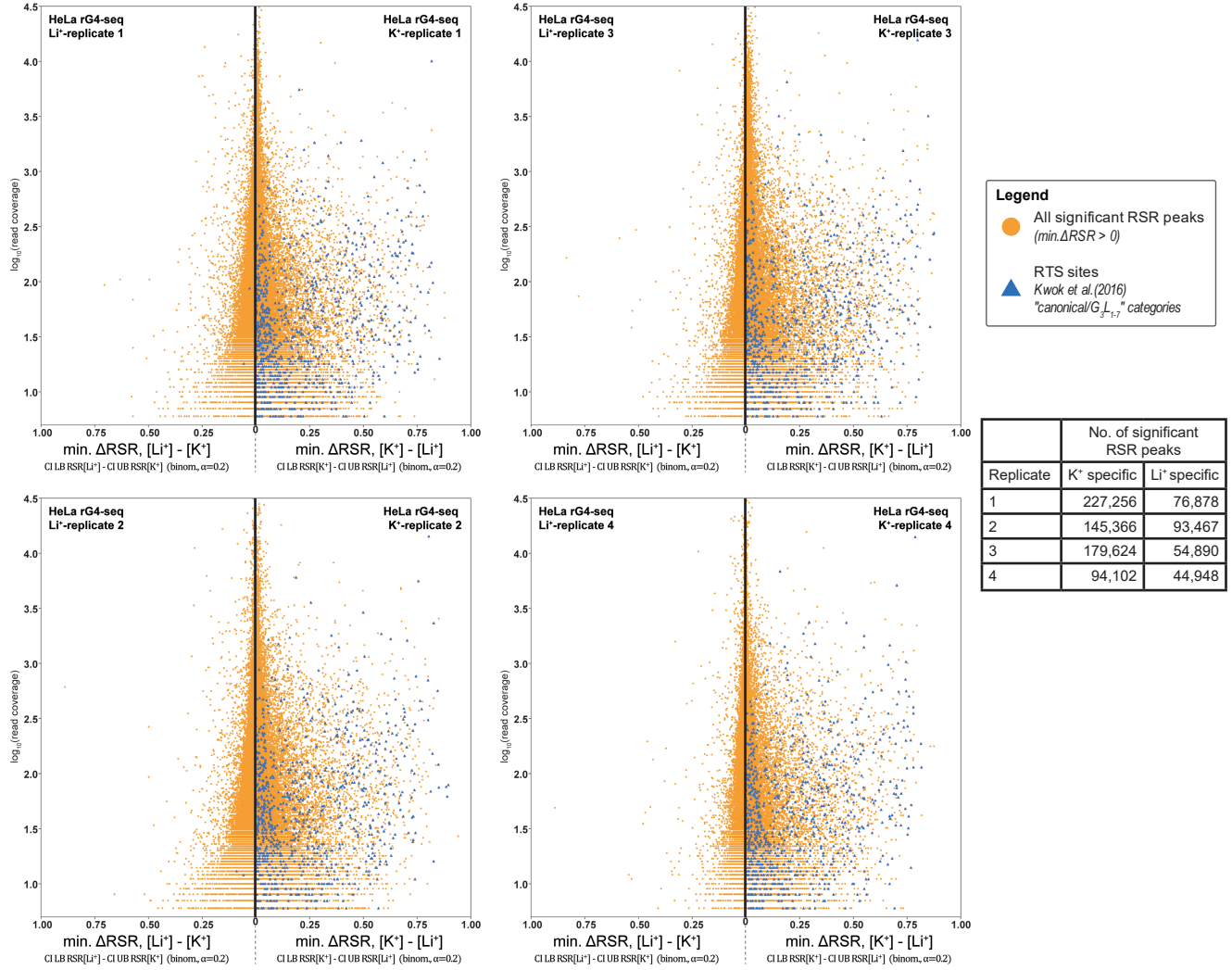


Figure S2

Transcriptome-wide significant RSR peaks (minimum $\Delta RSR > 0$) detected from the 4 replicates of HeLa rG4-seq dataset (pairwise comparison between K⁺/Li⁺ condition). Minimum ΔRSR values (indicating RTS effect strength) of RSR peaks were plotted against read coverage (logarithmic scale). Each datapoint corresponds to 1 RSR peak at 1 single-nucleotide genomic locus. RSR peaks coinciding with RTS sites in canonical/ G_3L_{1-7} reported by Kwok et al. (2016) are highlighted.

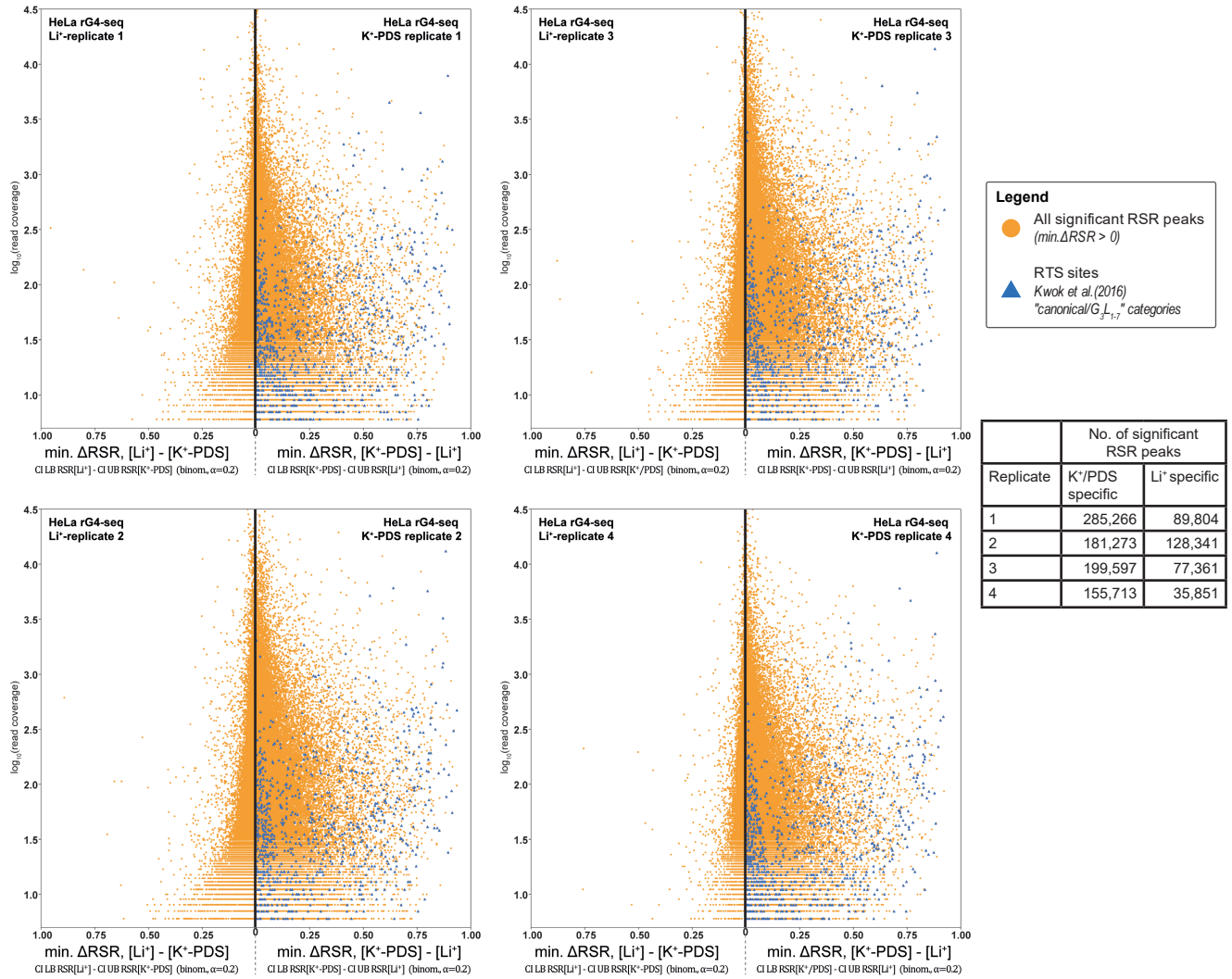


Figure S3

Transcriptome-wide significant RSR peaks (minimum $\Delta RSR > 0$) detected from the 4 replicates of HeLa rG4-seq dataset (pairwise comparison between K⁺-PDS/Li⁺ condition). Minimum ΔRSR values (indicating RTS effect strength) of RSR peaks were plotted against read coverage (logarithmic scale). Each datapoint corresponds to 1 RSR peak at 1 single-nucleotide genomic locus. RSR peaks coinciding with RTS sites in canonical/G₃L₁₋₇ reported by Kwok et al. (2016) are highlighted.

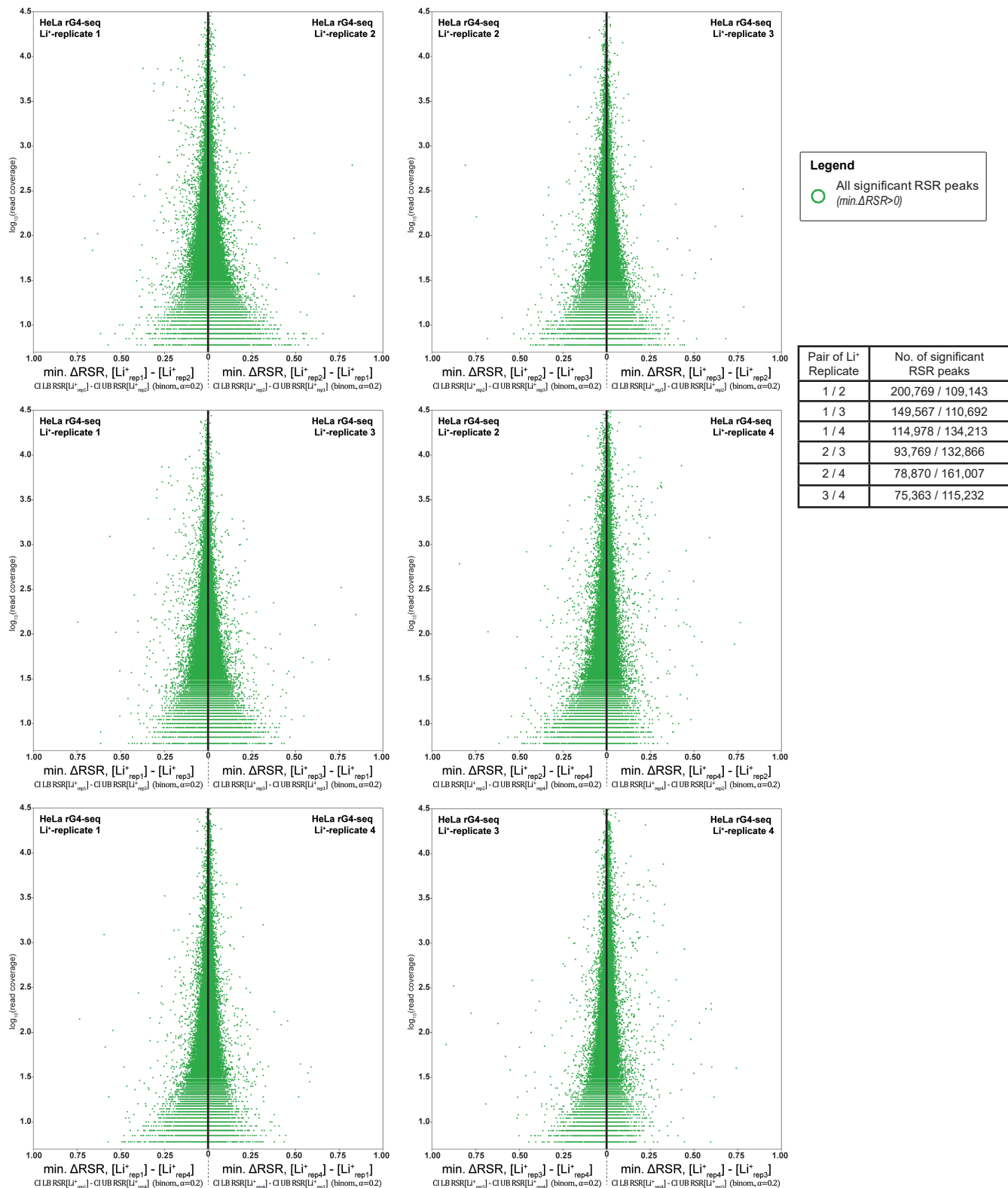


Figure S4

Transcriptome-wide significant RSR peaks (minimum $\Delta RSR > 0$) detected from pairwise comparisons between 4 replicates the Li⁺ HeLa rG4-seq dataset. Comparison between replicates of identical conditions implies that all detected RSR peaks originated from experimental variations.

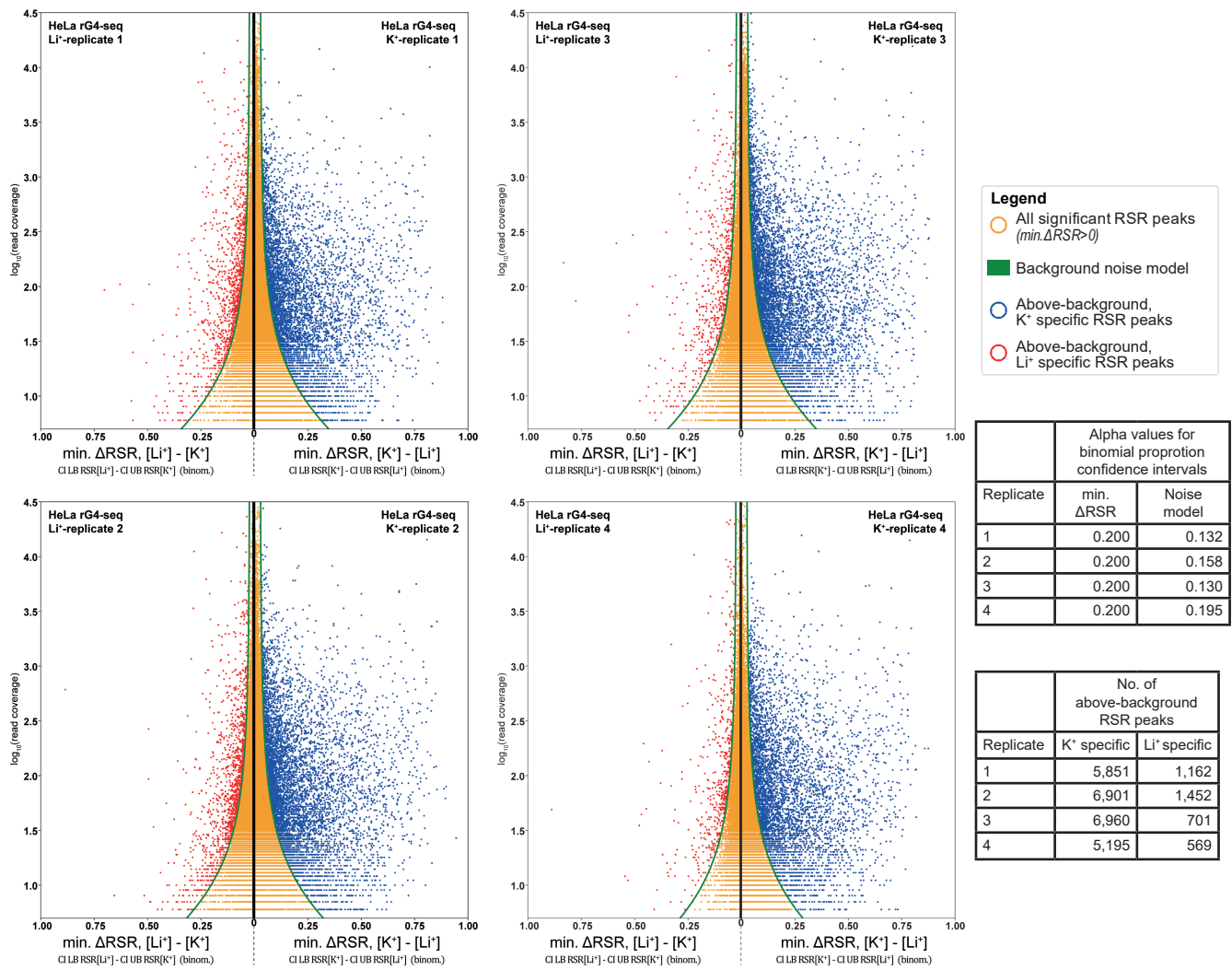


Figure S5

RSR peaks identified *ab initio* from pairwise comparison of 4 replicates of HeLa rG4-seq (K^+) and HeLa rG4-seq(Li^+) by applying the minimum ΔRSR metric scheme, sequence-based filtering scheme and fragmentation-associated noise model.

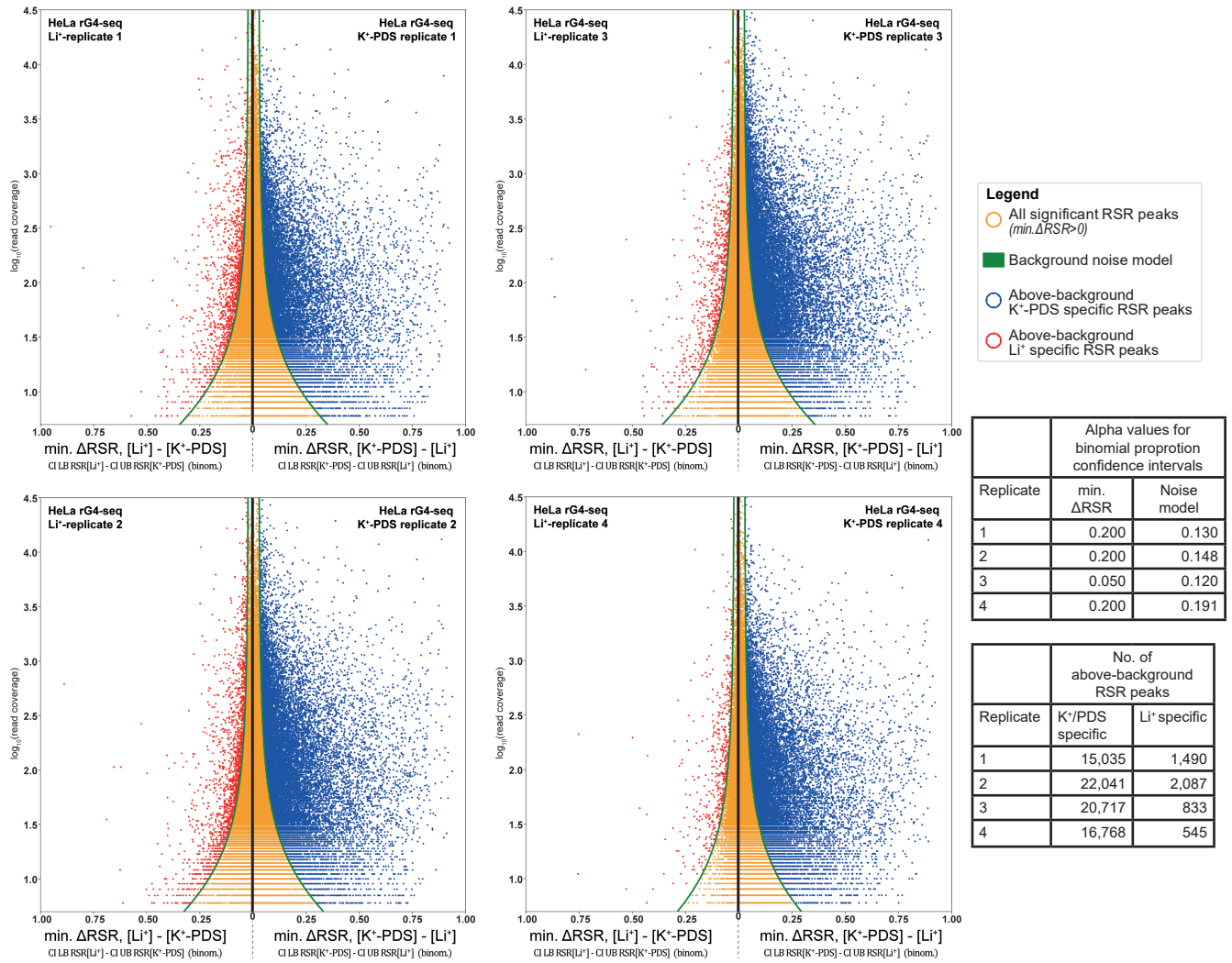


Figure S6

RSR peaks identified *ab initio* from pairwise comparison of 4 replicates of HeLa rG4-seq (K^+ -PDS) and HeLa rG4-seq(Li^+) by applying the minimum ΔRSR metric scheme, sequence-based filtering scheme and fragmentation-associated noise model.

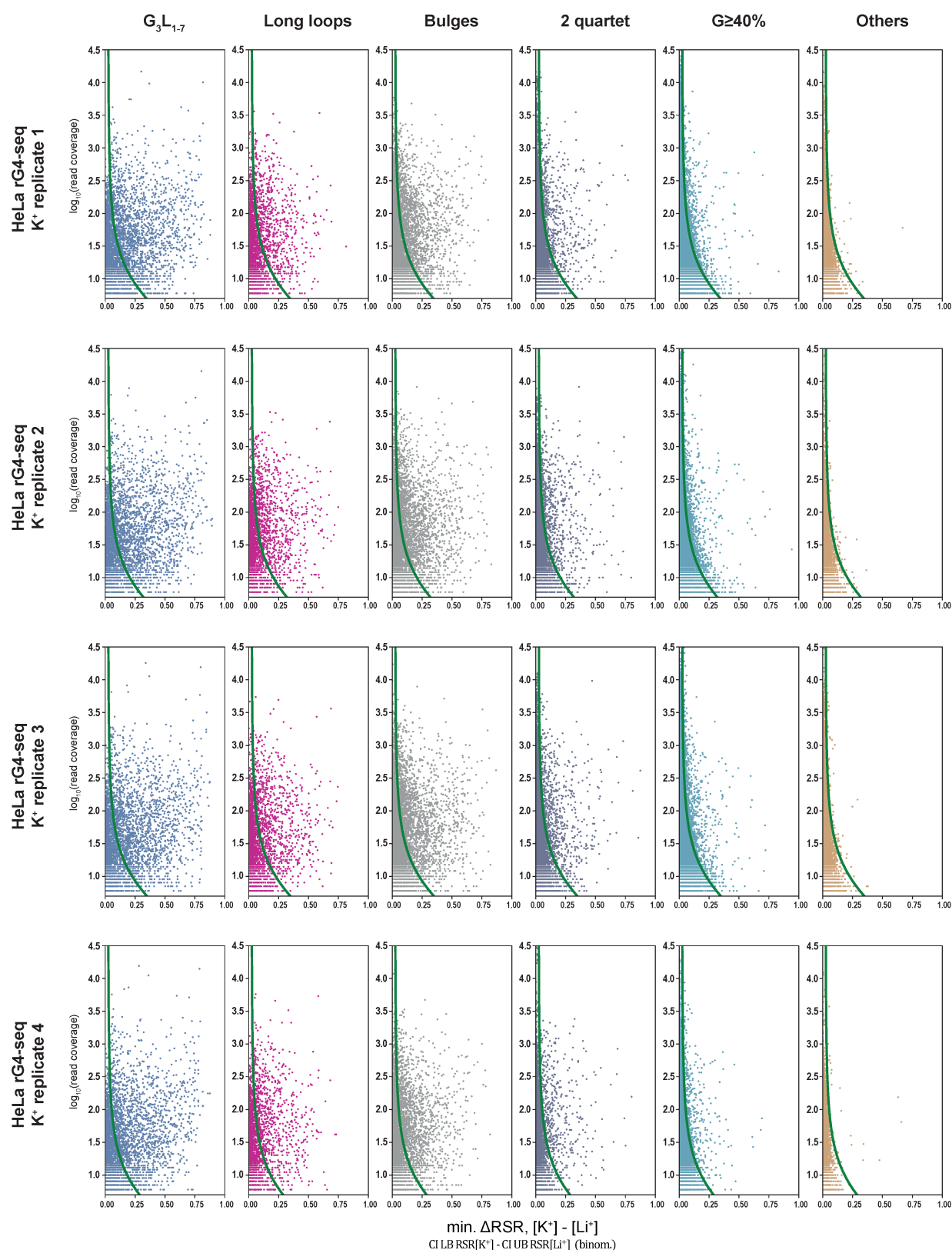


Figure S7

Significant ($\min. \Delta\text{RSR} > 0$) K^+ specific RSR peaks identified from the 4 replicates of HeLa rG4-seq (K^+) and HeLa rG4-seq(Li^+) (shown in Supplementary Figure S5) further categorized into the 6 structural subclasses (G_3L_{1-7} , long loops, 2-quartet, bulges, $\text{G} \geq 40\%$ and Others) based on the context of adjacent sequences. Green curves correspond to the background noise model applied to respective replicates.

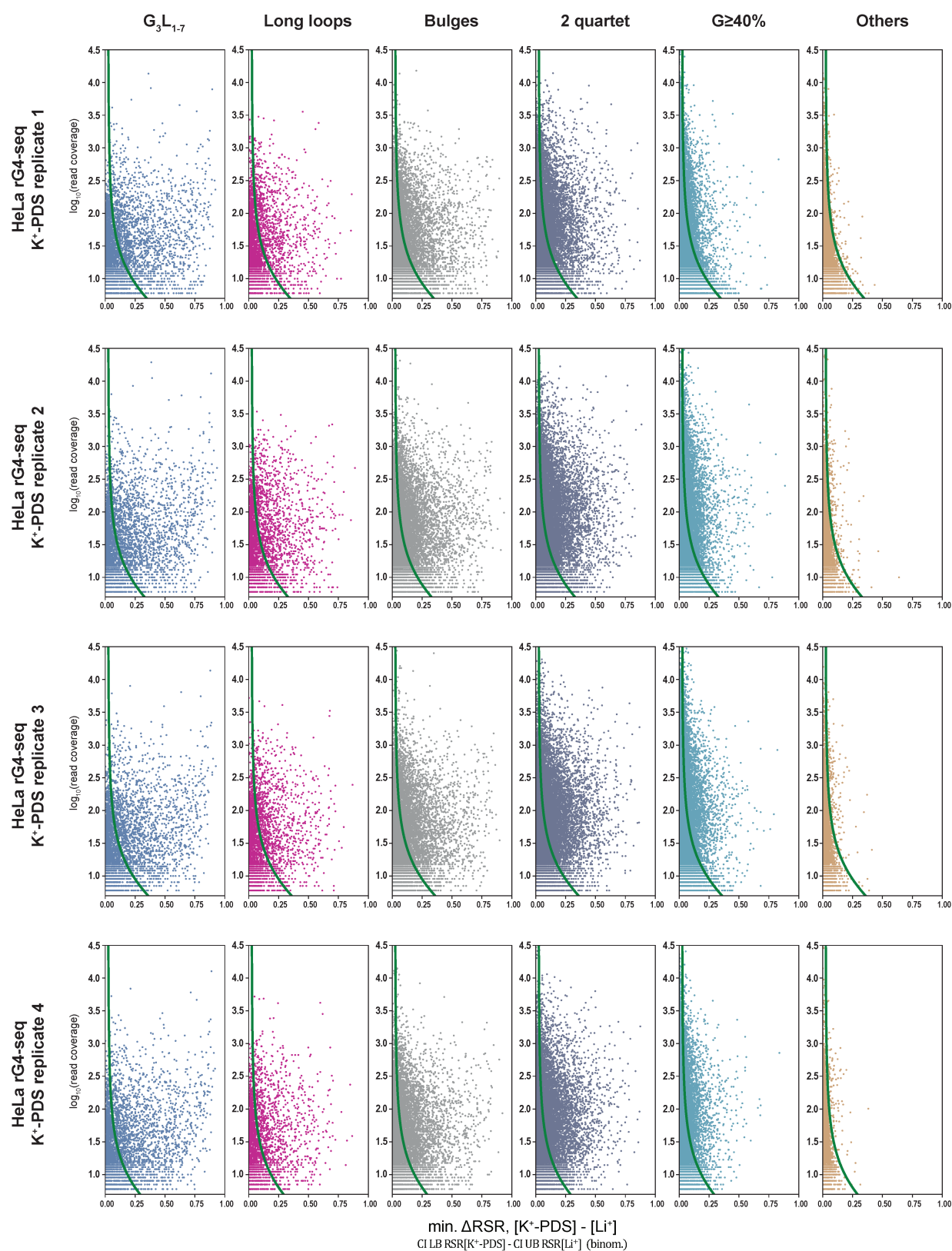


Figure S8

Significant ($\min. \Delta\text{RSR} > 0$) K⁺-PDS specific RSR peaks identified from the 4 replicates of HeLa rG4-seq (K⁺-PDS) and HeLa rG4-seq (Li⁺) (shown in Supplementary Figure S6) further categorized into the 6 structural subclasses (G_3L_{1-7} , long loops, 2-quartet, bulges, $G \geq 40\%$ and Others) based on the context of adjacent sequences. Green curves correspond to the background noise model applied to respective replicates.

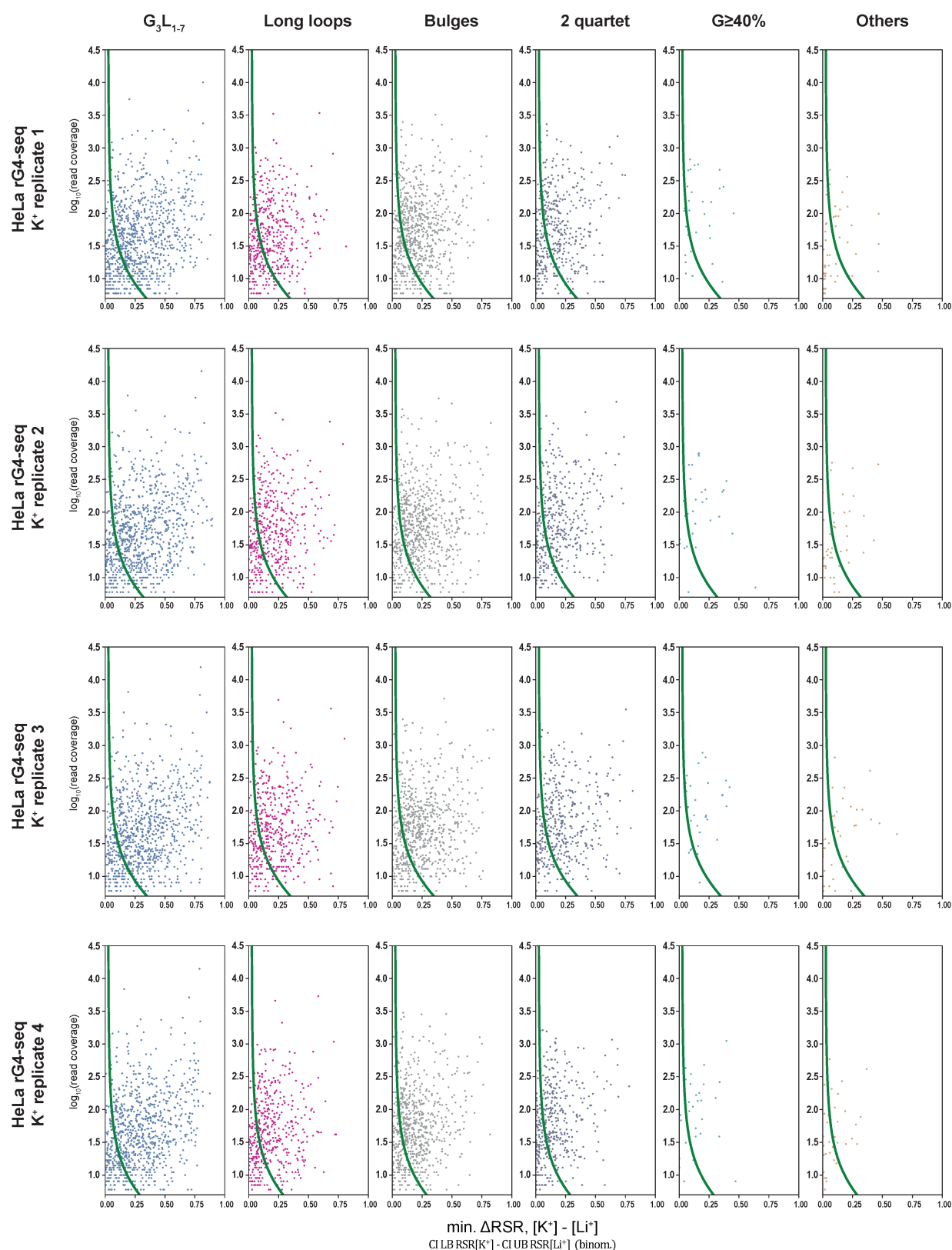


Figure S9

Significant ($\min \Delta\text{RSR} > 0$) K^+ specific RSR peaks identified from the 4 replicates of HeLa rG4-seq (K^+) and HeLa rG4-seq(Li^+) in this study that matched RTS sites (K^+) previously reported by Kwok et al. (2016). RSR peaks were categorized according to the structural subclass of the matching RTS sites. Green curves correspond to the background noise model applied to respective replicates. Non-significant ($\min. \Delta\text{RSR} \leq 0$) RSR peaks were not shown.

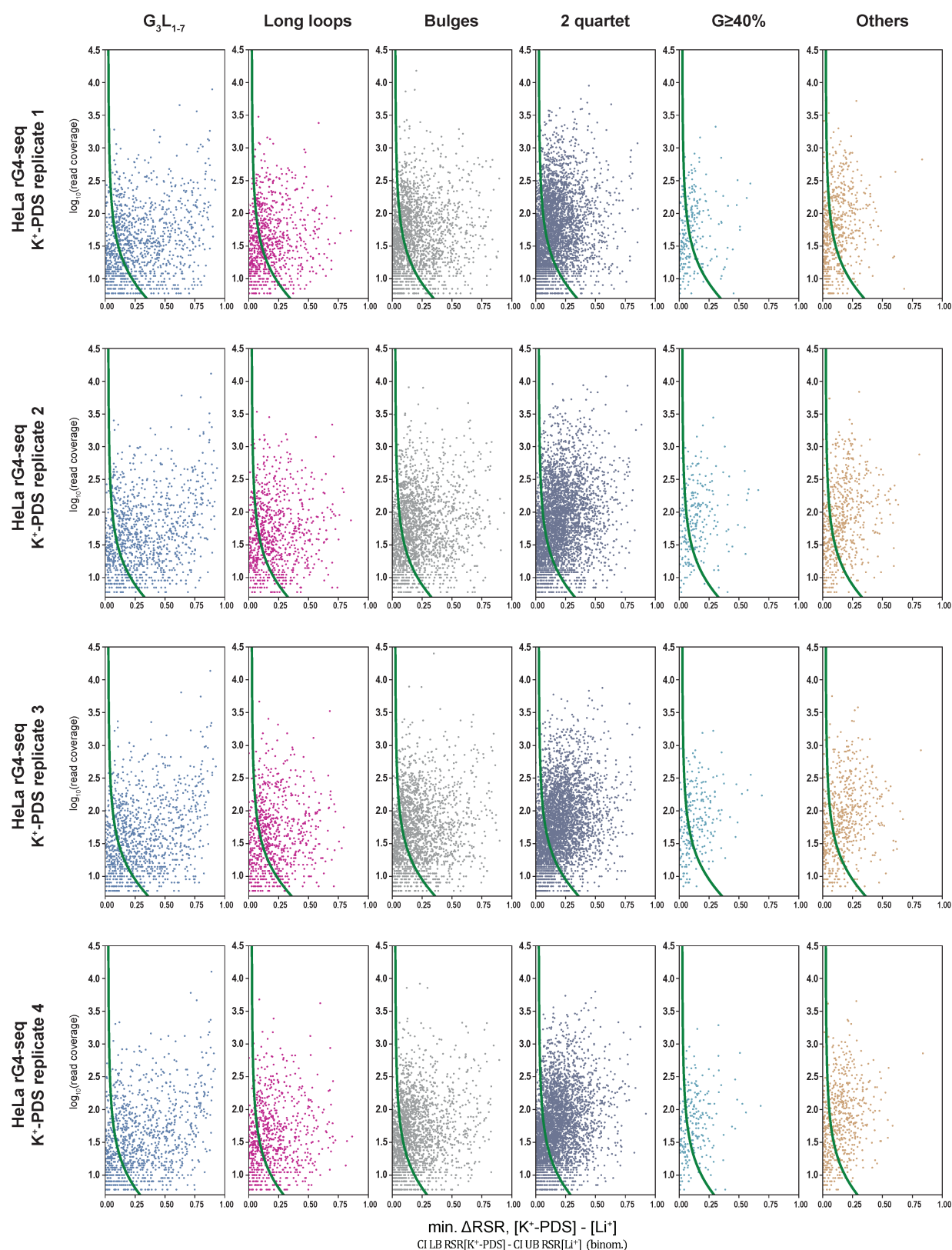


Figure S10

Significant ($\min. \Delta\text{RSR} > 0$) $\text{K}^+\text{-PDS}$ specific RSR peaks identified from the 4 replicates of HeLa rG4-seq ($\text{K}^+\text{-PDS}$) and HeLa rG4-seq (Li^+) in this study that matched RTS sites ($\text{K}^+\text{-PDS}$) previously reported by Kwok et al. (2016). RSR peaks were categorized according to the structural subclass of the matching RTS sites. Green curves correspond to the background noise model applied to respective replicates. Non-significant ($\min. \Delta\text{RSR} \leq 0$) RSR peaks were not shown.

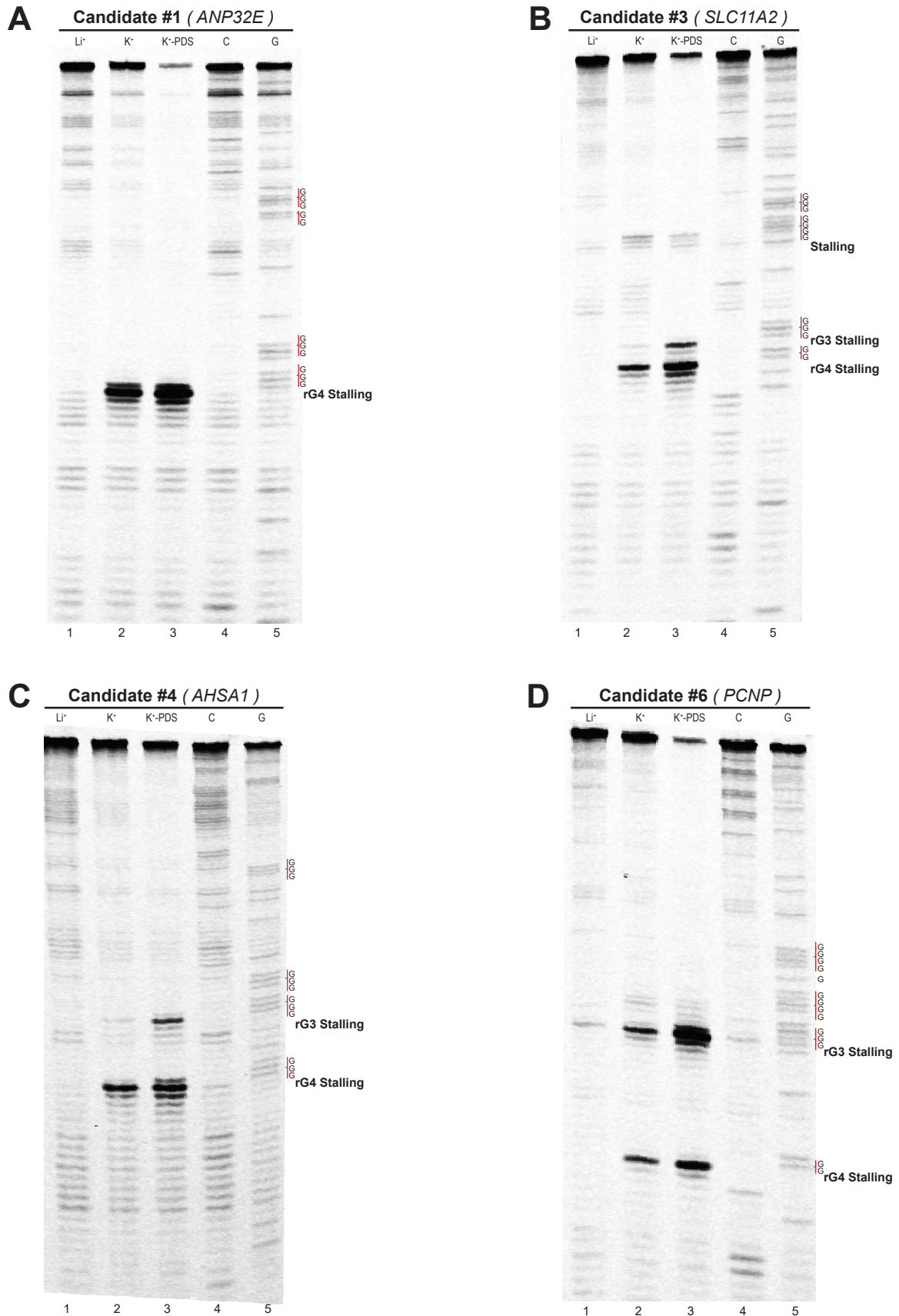


Figure S11

(a) RTS PAGE assay of a potential rG4 candidates on *ANP32E* gene indicated clear RTS at the 3' end of the 4th G-tract.

(b,c) RTS PAGE assay of two potential rG4 candidates on (b) *SLC11A2* gene (c) *AHSA1* gene indicated clear RTS at the 3' end of the 3rd and 4th G-tracts, respectively.

(d) A potential rG3 was initially suggested to form on *PCNP* gene based on findings from rG4-seq. RTS PAGE assay revealed a 4th G-tract 13 nt downstream of the 3rd G-tract, indicating that the region harbored a rG4 motif instead.

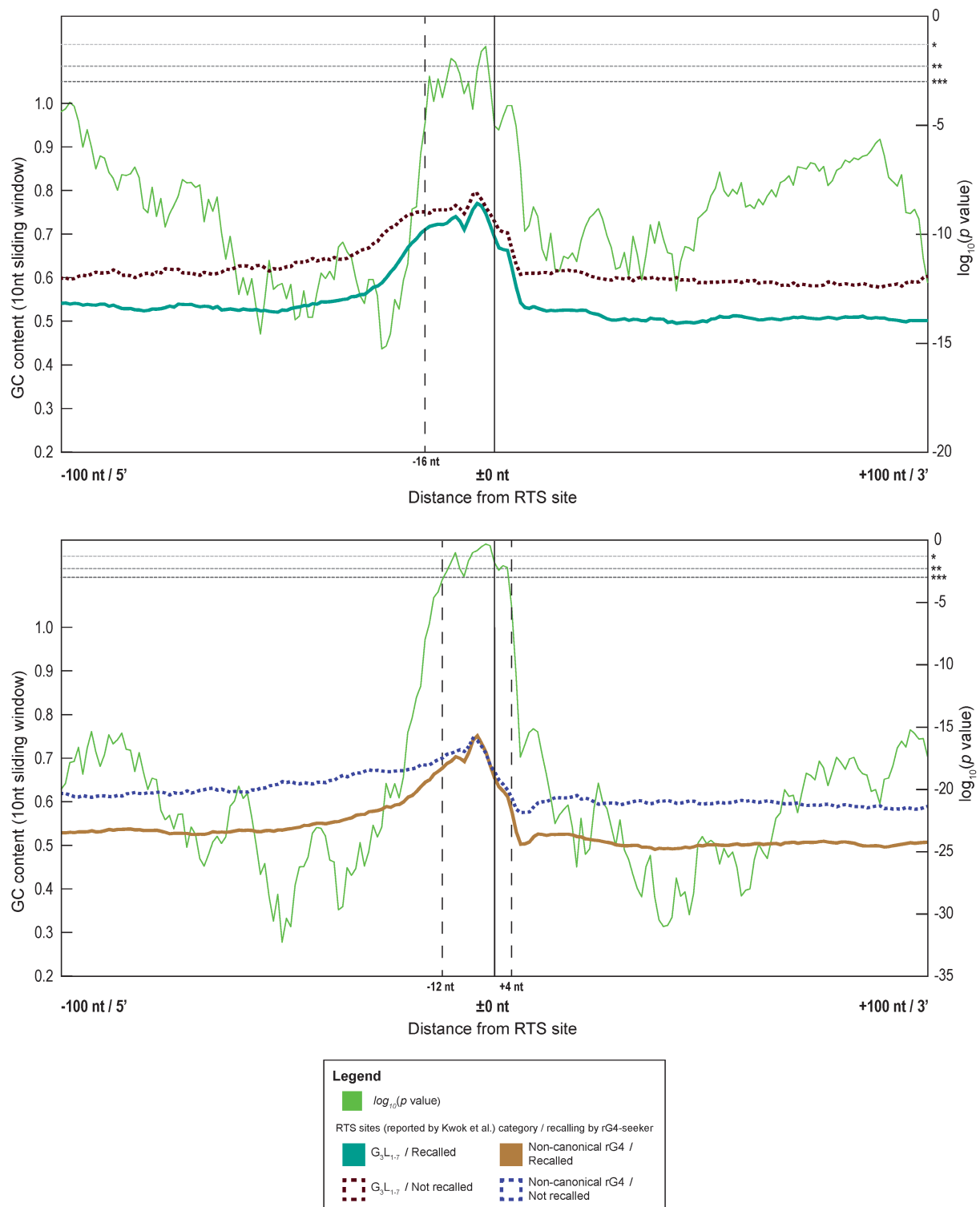


Figure S12

Average GC% (10 nt sliding windows) in the ± 100 nt region of the 3358 RTS sites (K^+) reported by Kwok et al. (2016), segregated based on their motif categories (canonical or non-canonical) and recall status by rG4-seeker. Mann-Whitney U test was applied to compare the differences in average GC% values between recalled and non-recalled RTS sites. Corresponding $\log_{10} p$ values were plotted as separate curves (*, **, *** = p -value < 0.01, 0.005 and 0.001 respectively).

Chromosome	Start	End	Strand	Gene name	3' Sequence (30nt)	RTS site location	RTS site Contains 'GGG' Motifs	Detected by Binomial test	Detected by min. ARSR scheme**
RTS site adjacent to G residues (35 sites)									
chr1	21070287	21070317	-	HP1BP3	AGTGCTGGGATTACAGGAGTGAGCCACTGT	chr1:21070287:-	No	Y	Y
chr1	150191011	150191041	-	ANP32E	GTATTTTCATGCAAATAAGTAAGGGTGGGT	chr1:150191011:-	Yes	Y	Y
chr1	180942946	180942976	-	STX6	TTACTTAAATGATTTGAGGGGTGGGAGGGA	chr1:180942946:-	Yes	Y	Y
chr1	185267080	185267110	-	IVNS1ABP	GTACACTTGTGAATAAAGAGGGTGGGTGGG	chr1:185267080:-	Yes	Y	Y
chr1	229773622	229773652	+	URB2	TGCAGCAGGTTGTGCTGCAGACAGGAGCTG	chr1:229773652:+	No		
chr10	50732243	50732273	-	ERCC6/PGBD3	TATGAGCTGAAGCCTCTGCCCAAGGGCGGG	chr10:50732243:-	Yes	Y	
chr11	17109477	17109507	-	PIK3C2A	TTGATAATATATCACTGGGACGGGGTGGGG	chr11:17109477:-	Yes	Y	Y
chr12	10758800	10758830	-	MAGOHB	AGGGGTTATTTGTCATTTACAGTATTGGGG	chr12:10758800:-	Yes	Y	Y
chr12	16500625	16500723	+	MGST1	GGGAGGGGCCAGGGTGGGTGGCAGATGGAAG	chr12:16500723:+	No		
chr12	16500635	16500733	+	MGST1	GGGTGGGTGGCAGATGGAAGACTTGGGGGG	chr12:16500733:+	Yes	Y	
chr14	81687271	81687499	-	GTF2A1	TCTCGGCGGCGGCGGCGGCGGCGGTGGTGG	chr14:81687271:-	No	Y	
chr14	74164495	74164525	+	DNAL1	AGTTTTCTTTTCTCTCTTCTTTTCAATCTG	chr14:74164525:+	No		
chr15	86291231	86291261	+	AKAP13	TAGATAGACCCTGCCTTAGTAGAGGGTGGG	chr15:86291261:+	Yes	Y	Y
chr16	19132439	19132469	+	ITPRIPL2	GGGATAAAGCATGTATAAGTTGGGAGAGGG	chr16:19132469:+	Yes	Y	Y
chr16	85707376	85707406	+	KIAA0182	GTGACAGTCATGTGCACACATGGGCGGGGG	chr16:85707406:+	Yes	Y	Y
chr17	3715611	3715641	-	C17orf85	TTTGGGGTTGATTTTTGTGCTGGGGTGGGA	chr17:3715611:-	Yes	Y	Y
chr17	49257909	49257939	-	MBTD1	GAGGTGGCTTAGAACTGAGGGCGGGTGGG	chr17:49257909:-	Yes	Y	Y
chr17	60023147	60023177	-	MED13	CGATGTACAGTTTAACGGGGATAGAGGGGG	chr17:60023147:-	Yes	Y	Y
chr17	7210424	7210876	+	EIF5A	CGCTTGCGCAGTGCGGGGGTGGAGGGCGGA	chr17:7210876:+	Yes	Y	Y
chr17	40128540	40128570	+	CNP	GTCCACCCCCGCCTCCCTCCCCTGCCCTCG	chr17:40128570:+	No		
chr19	59028606	59028636	-	ZBTB45	CTGCCCACCCCTGTGCCCCCGCCACTCGCA	chr19:59028606:-	No		
chr2	68406110	68406140	-	PPP3R1	TTTTTTTTTTTTAGTTTGTGTGTGGGGGTG	chr2:68406110:-	Yes		

chr2	201676698	201676923	+	BZW1	GGGTAGCGGCGGCCCGGGTGGGGAGGTGGG	chr2:201676923:+	Yes	Y	Y
chr22	21356311	21356341	+	THAP7-AS1	CGGCCCGTTGTCGCCCCAACCCCGTCCCAG	chr22:21356341:+	No		
chr3	152017907	152017937	+	MBNL1	TGGTTGTTGCTCTTTTTTGGGGGGGTTGGG	chr3:152017937:+	Yes	Y	Y
chr5	126172247	126172277	+	LMNB1	TTTTTTAAGTTCTTATGAGGAGGGGAGGGT	chr5:126172277:+	Yes	Y	Y
chr6	43586704	43586734	+	POLH	GGGGTTCTATATTTAGTTTGAAGAGGTGGG	chr6:43586734:+	Yes	Y	
chr6	145172425	145172455	+	UTRN	ATGTATACAGCATTGGGAAAGTGGGTGGGG	chr6:145172455:+	Yes	Y	Y
chr7	97851053	97851716	-	TECPR1	CAGCCTCCCCTTCGCAGGTGACTGCTGGTA	chr7:97851053:-	No		
chr7	94298466	94298496	+	PEG10	ATAATCATAAGCATTTTAGGGTGGGAGGGA	chr7:94298496:+	Yes	Y	Y
chr9	14086231	14086261	-	NFIB	CATATATATATATTCTGGGGTGGGTGGGAG	chr9:14086231:-	Yes	Y	Y
chr9	2193003	2193033	+	SMARCA2	TGGGTGGATAGTATATTTCTATGGGTGGGT	chr9:2193033:+	Yes	Y	Y
chrX	150158023	150158053	+	HMGB3	GTAACATTTTATCCAGGTTGGGGTGAGGGG	chrX:150158053:+	Yes	Y	Y
RTS site non-adjacent to G residues (7 sites)									
chr1	202554249	202554279	+	PPP1R12B	AGCAGCTAGGACTGCAGGTGTGCACCACCA	chr1:202554279:+	No		
chr15	56735938	56735968	-	MNS1	AAGAAACGTGAGGAGATGGAAGAAGAAAAC	chr15:56735938:-	No		
chr16	58554140	58554170	-	CNOT1	CCTAAAGCCCACCCCTACCCTACCCCCCCC	chr16:58554140:-	No	Y	
chr19	11033127	11033157	+	CARM1	CCCCTGCAGGTCCCCCCCCGCCCCCCCCT	chr19:11033157:+	No		
chr19	56152393	56152413	+	ZNF580	CCTCGCACCCCCGCGCCCCC	chr19:56152413:+	No		
chr3	53319128	53319158	-	DCP1A	TTTGTGTGCCACCCCCACCCCCAGGGTCT	chr3:53319128:-	Yes		
chr3	15296907	15296937	+	LOC100505696	GTCCCTCCTACCCTCATCCCCCGCATCCC	chr3:15296937:+	No		
chr9	112810945	112810975	+	AKAP2	CTCCAGCGCGCCCGGAGGCTACCACTCCCT	chr9:112810975:+	No		

Table S1

Details of 42 “Others” RTS sites previously reported in Kwok et al. (2016) and simultaneously recalled with RSR metric and binomial test / minimum Δ RSR scheme from both rG4-seq (K^+) and rG4-seq (K^+ -PDS). Genomic coordinates were corresponding to GRCh37/hg19 human reference genome. Properties of the RTS sites (adjacency to G residues / containing ‘GGG’ motifs) and their recalling status were shown in the table.

RTS sites (K ⁺) reported by Kwok et al. (2016)	G ₃ L ₁₋₇			Long loops			Bulges			2 quartet			G≥40%			Others		
Status of matching RSR peak	Significant (min. ΔRSR>0), Above-background	Significant (min. ΔRSR>0), Below-background	Not significant (min. ΔRSR≤0)	Significant (min. ΔRSR>0), Above-background	Significant (min. ΔRSR>0), Below-background	Not significant (min. ΔRSR≤0)	Significant (min. ΔRSR>0), Above-background	Significant (min. ΔRSR>0), Below-background	Not significant (min. ΔRSR≤0)	Significant (min. ΔRSR>0), Above-background	Significant (min. ΔRSR>0), Below-background	Not significant (min. ΔRSR≤0)	Significant (min. ΔRSR>0), Above-background	Significant (min. ΔRSR>0), Below-background	Not significant (min. ΔRSR≤0)	Significant (min. ΔRSR>0), Above-background	Significant (min. ΔRSR>0), Below-background	Not significant (min. ΔRSR≤0)
K ⁺ replicate 1	704 (61.6%)	210 (18.4%)	229 (20.0%)	312 (52.6%)	166 (28.0%)	115 (19.4%)	554 (59.8%)	194 (21.0%)	178 (19.2%)	295 (46.5%)	132 (20.8%)	208 (32.8%)	22 (36.1%)	10 (16.4%)	29 (47.5%)	21 (4.6%)	38 (8.3%)	401 (87.2%)
K ⁺ replicate 2	717 (62.7%)	178 (15.6%)	248 (21.7%)	335 (56.5%)	116 (19.6%)	142 (23.9%)	583 (63.0%)	131 (14.1%)	212 (22.9%)	297 (46.8%)	112 (17.6%)	226 (35.6%)	24 (39.3%)	8 (13.1%)	29 (47.5%)	21 (4.6%)	24 (5.2%)	415 (90.2%)
K ⁺ replicate 3	712 (62.3%)	181 (15.8%)	250 (21.9%)	348 (58.7%)	119 (20.1%)	126 (21.2%)	576 (62.2%)	171 (18.5%)	179 (19.3%)	322 (50.7%)	99 (15.6%)	214 (33.7%)	26 (42.6%)	5 (8.2%)	30 (49.2%)	22 (4.8%)	21 (4.6%)	417 (90.7%)
K ⁺ replicate 4	695 (60.8%)	170 (14.9%)	278 (24.3%)	327 (55.1%)	128 (21.6%)	138 (23.3%)	534 (57.7%)	175 (18.9%)	217 (23.4%)	282 (44.4%)	128 (20.2%)	225 (35.4%)	24 (39.3%)	7 (11.5%)	30 (49.2%)	17 (3.7%)	18 (3.9%)	425 (92.4%)

Table S2
 Status of RSR peaks that matched with RTS sites (K⁺) reported by Kwok et al. (2016).

RTS sites (K ⁺ -PDS) reported by Kwok et al. (2016)	G ₃ L ₁₋₇			Long loops			Bulges			2 quartet			G≥40%			Others		
Status of matching RSR peak	Significant (min. ΔRSR>0), Above-background	Significant (min. ΔRSR>0), Below-background	Not significant (min. ΔRSR≤0)	Significant (min. ΔRSR>0), Above-background	Significant (min. ΔRSR>0), Below-background	Not significant (min. ΔRSR≤0)	Significant (min. ΔRSR>0), Above-background	Significant (min. ΔRSR>0), Below-background	Not significant (min. ΔRSR≤0)	Significant (min. ΔRSR>0), Above-background	Significant (min. ΔRSR>0), Below-background	Not significant (min. ΔRSR≤0)	Significant (min. ΔRSR>0), Above-background	Significant (min. ΔRSR>0), Below-background	Not significant (min. ΔRSR≤0)	Significant (min. ΔRSR>0), Above-background	Significant (min. ΔRSR>0), Below-background	Not significant (min. ΔRSR≤0)
K ⁺ -PDS replicate 1	824 (51.0%)	339 (21.0%)	453 (28.0%)	524 (42.8%)	332 (27.1%)	368 (30.1%)	1,308 (46.3%)	780 (27.6%)	735 (26.0%)	2,444 (47.1%)	1,368 (26.4%)	1,379 (26.6%)	143 (32.7%)	120 (27.5%)	174 (39.8%)	342 (16.7%)	323 (15.8%)	1,382 (67.5%)
K ⁺ -PDS replicate 2	841 (52.0%)	267 (16.5%)	508 (31.4%)	601 (49.1%)	247 (20.2%)	376 (30.7%)	1,469 (52.0%)	548 (19.4%)	806 (28.6%)	2,879 (55.5%)	929 (17.9%)	1,383 (26.6%)	167 (38.2%)	82 (18.8%)	188 (43.0%)	432 (21.1%)	207 (10.1%)	1,408 (68.8%)
K ⁺ -PDS replicate 3	824 (51.0%)	310 (19.2%)	482 (29.8%)	561 (45.8%)	264 (21.6%)	399 (32.6%)	1,417 (50.2%)	606 (21.5%)	800 (28.3%)	2,790 (53.7%)	1,063 (20.5%)	1,338 (25.8%)	157 (35.9%)	101 (23.1%)	179 (41.0%)	415 (20.3%)	212 (10.4%)	1,420 (69.4%)
K ⁺ -PDS replicate 4	808 (50.0%)	274 (17.0%)	534 (33.0%)	549 (44.9%)	246 (20.1%)	429 (35.0%)	1,356 (48.0%)	611 (21.6%)	856 (30.3%)	2,661 (51.3%)	1,048 (20.2%)	1,482 (28.5%)	156 (35.7%)	84 (19.2%)	197 (45.1%)	400 (19.5%)	209 (10.2%)	1,438 (70.2%)

Table S3
 Status of RSR peaks that matched with RTS sites (K⁺-PDS) reported by Kwok et al. (2016).

TablMin. Read coverage	rg4-seq condition	#Replicate	\sum (sequenced positions)	\sum (sequenced positions containing ≥ 1 read start)	$P(B)$	\sum (read coverage of sequenced positions containing ≥ 1 read start)	\sum (read starts in sequenced positions)	$P(A \cap B)$	$P(A B)$
$\geq 6x$	K ⁺	1	43,446,617	15,559,362	0.3581	3,565,444,556	63,742,568	0.0179	0.0500
$\geq 6x$	K ⁺	2	41,216,131	13,017,953	0.3158	3,475,638,448	55,074,928	0.0158	0.0500
$\geq 6x$	K ⁺	3	42,105,455	13,507,453	0.3208	2,938,246,465	53,703,833	0.0183	0.0570
$\geq 6x$	K ⁺	4	52,722,179	18,186,769	0.3450	4,335,282,487	71,534,010	0.0165	0.0478
$\geq 6x$	K ⁺ -PDS	1	42,869,611	14,025,229	0.3272	3,289,338,871	57,789,844	0.0176	0.0538
$\geq 6x$	K ⁺ -PDS	2	43,987,073	13,504,356	0.3070	4,094,271,905	60,450,721	0.0148	0.0482
$\geq 6x$	K ⁺ -PDS	3	45,369,082	14,425,694	0.3180	3,571,228,263	58,973,001	0.0165	0.0519
$\geq 6x$	K ⁺ -PDS	4	48,887,275	16,817,154	0.3440	3,588,040,463	62,777,600	0.0175	0.0509
$\geq 6x$	Li ⁺	1	51,853,328	18,478,171	0.3564	5,911,086,239	94,523,439	0.0160	0.0449
$\geq 6x$	Li ⁺	2	44,667,183	14,294,298	0.3200	4,498,217,619	68,307,246	0.0152	0.0475
$\geq 6x$	Li ⁺	3	46,364,524	14,839,833	0.3201	3,945,219,400	60,734,921	0.0154	0.0481
$\geq 6x$	Li ⁺	4	61,746,013	22,473,562	0.3640	6,364,155,240	102,464,720	0.0161	0.0442
$\geq 2048x$	K ⁺	1	205,377	195,888	0.9538	1,025,436,370	14,098,748	0.0137	0.0144
$\geq 2048x$	K ⁺	2	221,608	210,082	0.9480	1,135,915,016	13,551,271	0.0119	0.0126
$\geq 2048x$	K ⁺	3	171,093	161,626	0.9447	868,319,850	11,693,007	0.0135	0.0143
$\geq 2048x$	K ⁺	4	246,912	235,807	0.9550	1,263,548,976	16,413,174	0.0130	0.0136
$\geq 2048x$	K ⁺ -PDS	1	188,137	179,164	0.9523	960,864,841	12,600,469	0.0131	0.0138
$\geq 2048x$	K ⁺ -PDS	2	263,891	250,757	0.9502	1,393,577,813	15,607,667	0.0112	0.0118
$\geq 2048x$	K ⁺ -PDS	3	210,136	200,039	0.9520	1,103,055,047	13,721,284	0.0124	0.0130
$\geq 2048x$	K ⁺ -PDS	4	197,311	187,999	0.9528	978,523,049	13,190,069	0.0135	0.0142
$\geq 2048x$	Li ⁺	1	376,146	362,479	0.9637	2,057,673,637	26,572,792	0.0129	0.0134
$\geq 2048x$	Li ⁺	2	299,899	286,568	0.9555	1,615,155,435	19,049,791	0.0118	0.0123
$\geq 2048x$	Li ⁺	3	240,977	229,948	0.9542	1,308,568,932	15,330,434	0.0117	0.0123
$\geq 2048x$	Li ⁺	4	396,186	382,689	0.9659	2,082,612,795	27,703,361	0.0133	0.0138

Table S4

Raw number figures for deriving the conditional probability $P(A|B)$ for statistical modelling of fragmentation-associated background noise, where:

A: receiving 1 read start per 1x read coverage

B: receiving at least 1 read start

rG4-seq condition	#Replicate	Average aligned read length	1
			<i>Average aligned read length</i>
K ⁺	1	71	0.014085
K ⁺	2	82	0.012195
K ⁺	3	72	0.013889
K ⁺	4	76	0.013158
K ⁺ -PDS	1	74	0.013514
K ⁺ -PDS	2	87	0.011494
K ⁺ -PDS	3	79	0.012658
K ⁺ -PDS	4	73	0.013699
Li ⁺	1	75	0.013333
Li ⁺	2	82	0.012195
Li ⁺	3	83	0.012048
Li ⁺	4	74	0.013514

Table S5

Statistics of averaged aligned read lengths in HeLa rG4-seq datasets